Nanodynamics of Ferroelectric Ultrathin Films

Qingteng Zhang, R. Herchig, and I. Ponomareva

Phys. Rev. Lett. **107**, 177601 — Published 19 October 2011

DOI: 10.1103/PhysRevLett.107.177601

Nanodynamics of ferroelectric ultrathin films

Qingteng Zhang, R. Herchig, and I. Ponomareva*

Department of Physics, University of South Florida, Tampa, Florida 33620, USA

(Dated: September 14, 2011)

Abstract

The nanodynamics of ferroelectric ultrathin films made of $PbTi_{0.6}Zr_{0.4}TiO_3$ alloy is explored via the use of a first-principles-based technique. Our atomistic simulations predict that the nanostripe domains which constitute the ground state of ferroelectric ultrathin films under most of electric boundary conditions oscillate under a driving *ac*-field. Furthermore, we found that the atomically thin wall, or nanowall, that separates the nanodomains with different polarization directions behaves as an elastic object and has a mass associated with it. The nanowall mass is size-dependent and gives rise to a unique size-driven transition from resonance to relaxational dynamics in ultrathin films. A general theory of nanodynamics in such films is developed and used to explain all computational findings. In addition, we found an unusual dynamical coupling between nanodomains and mechanical deformations that could potentially be used in ultrasensitive electromechanical nanosensors.

PACS numbers: 77.80.Fm, 77.55.fg, 77.55.hj

Nanosize objects are known to have properties that are very different from their bulk counterparts. For example, ferroelectric nanostructures exhibit a variety of dipole patterns and states that are prohibited in the bulk [1–4]. Such nanostructures have become a subject of intense scientific and technological interest recently, thanks to their potential for device miniaturization [5, 6] and a variety of unusual phenomena [7, 8]. For example, nanoscale ferroelectric films and superlattices can exhibit nanostripes that are nanoscopic regions of "up" and "down" polarizations [2, 9, 10]. Interestingly, the nanostripes size and periodicity depend on the film thickness and follow the Kittel law down to thicknesses of just a few unit cells [11]. The nanostripes were predicted to have an unusual evolution under applied *dc* electric fields that includes the formation of nanobubbles [12]. A recent study [10] has reported that the velocity of the nanodomain walls that separate the nanostripes of the "up" and "down" polarization direction does not follow the Merz's law [13] that governs dynamics of larger domains [13, 14]. These recent findings seem to suggest that, while the static properties (such as nanodomain morphology at equilibrium) may follow the general trends and laws for ferroelectric domains, their dynamical properties deviate substantially. Such dynamical properties at nanoscale are of technological importance since they are at the heart of polarization switching [5, 6] (and, therefore, ultradense ferroelectric memory technology) and contribute to most of the materials responses such as dielectric and piezoelectric responses [15] (and therefore may play an important role in nanoscale ferroelectric sensors, actuators and others). Given the need for device miniaturization and strong deviation of ferroelectrics nanoscale dynamics from the dynamics of their macroscopic counterparts, the deep atomistic knowledge of ferroelectrics *nanodynamics* is highly desirable. In particular, one may wonder if and how the intrinsic dynamics of ferroelectric domains will change at nanoscale. Is a nanowall (the area that separates nanodomains of different polarization direction) an elastic object and will it follow the dynamical models developed for these objects? What is the characteristic frequency range for the nanostripes dynamics and how does it scale with their size? What type of intrinsic dynamics is associated with nanowalls and how different is it from the dynamics of larger domains? Are there any novel dynamical phenomena associated with nanoscale? To answer the questions about intrinsic fundamental dynamics of ferroelectric nanodomains one needs to subject these domains to a driving *ac*-field of sub-switching amplitude, which is the amplitude smaller than the coercive field. To the best of our knowledge, such studies have not been carried out for nanostripes which

has led to a gap in our understanding of the intrinsic dynamics of nanodomains.

In this Letter we take advantage of accurate first-principle-based simulations to reveal the intrinsic dynamics of nanodomains. We first demonstrate that the nanodomain walls oscillate under driving *ac*-field of sub-switching amplitude, which brings such nanowalls into the general class of objects with oscillatory dynamics. Secondly, we reveal that nanowalls can exhibit two types of intrinsic dynamics (resonance and relaxation) at the same frequencies. This is just the opposite of our current understanding of larger scale domain walls, where we expect resonance dynamics at high-frequencies and electric fields and relaxational dynamics (domain wall creep) at lower frequencies and electric fields. Thirdly, we prove that at nanoscale the dynamics is determined by the domain size which manifests itself via a unique size-driven transition from relaxational to resonance dynamics.

We used classical molecular dynamics (MD) with the force-field derived from first-principles-based effective Hamiltonian [16–18] to investigate nine ferroelectric ultrathin films made of $PbTi_{0.6}Zr_{0.4}TiO_3$ ferroelectric alloy and with thicknesses ranging from 2 to 20 nm. The degrees of freedom for the Hamiltonian include a local soft mode which is proportional to the local dipole moment, homogeneous and inhomogeneous strain variables [26]. This approach has been successfully applied to study static and dynamical properties of $PbTi_xZr_{1-x}TiO_3$ alloys [3, 4, 9, 19]. We simulate films grown along [001] direction and subject to epitaxial compressive strain and realistic partial screening of the surface charge. Technically, we model compressive strain of -2.64% by freezing some components of the homogeneous strain tensor [9], while the total surface charge is screened by 84% using the computational approach of Ref. [18]. In our setup x, y and z-directions are chosen along [100], [010], and [001] crystallographic directions with z-direction being perpendicular to the film. Periodic boundary conditions are applied along the x- and y-directions. The films were first annealed from T =2000 K down to T =10 K in steps of ΔT =100 K. For each temperature we equilibrate the dipoles by simulating NPT ensemble using MD with Evans-Hoover thermostat and barostat mimicked via PV term in the effective Hamiltonian [20, 21]. Technically we used 40,000 MD steps with each step being 0.5 fs. Ground state dipole patterns of these films consist of periodic nanostripe domains of alternating polarization (180° domains). The morphology of these nanostripes is in excellent agreement with experimental findings [2] and given in Fig.1. An average out-of-plane component of the local dipole $< q_z >$ is the key quantity for this study and is shown in Fig.1(b). Inside a domain the dipole's magnitude

is nonuniform with the longest (shortest) dipoles found in the center (far end) of a domain. This pattern is a consequence of a film's tendency to minimize the polarization gradient through the adjustment of the dipole's magnitude. As the film thickness increases so does the magnitude of the dipoles, while the shape of the profile flattens. The nanowalls are one unit cell thick. The lateral size of the domains ranges from 1.6 to 5 nm and follows the Kittel square root law (see Fig.1(e)). To study the oscillatory dynamics of these nanowalls we turn to non-equilibrium MD [20] and apply sub-switching *ac* electric field with frequencies 1 GHz - 4 THz along the film's out-of-plane direction at $T = 10$ K [27]. Under the electric field, the dipoles near the nanowalls flip to align with the field which leads to a sideways motion of the domain wall. Since the direction of the electric field alternates, so does the direction of the domain wall motion resulting in the oscillatory dynamics of the nanowall. Typically we simulate at least thirty periods of *ac* field to achieve steady state.

We first focus on the oscillatory dynamics in the thinnest film and trace the time evolution of the average nanowall's displacement from its equilibrium position ΔX. This displacement is obtained from the count of dipoles flipped during the simulation. After the first few transient oscillations the dynamics reaches its steady state where the displacement follows the harmonic solution $\Delta X = X \sin(\omega t + \phi)$, indicating that the nanowall moves as an elastic object. Here X is the amplitude of the nanowall's displacement, ω is the *ac* field frequency, t is time, and ϕ is the phase-shift with respect to the electric field. By analyzing the nanowall's response to an electric field of different frequencies we obtain dependences $X(\omega)$ and $\phi(\omega)$ given in Fig.2, and then combine them into a complex response function $\eta(w) = X \cos\phi + iX \sin\phi$. Below 0.3 THz the domain response is independent of the frequency (Fig.2(a)) with the nanowalls oscillating in phase with the electric field (Fig.2(b)). Above 1.5 THz the nanowalls have difficulty following the electric field as indicated by the drastic decrease in the amplitude X and increase in phase-shift ϕ. Surprisingly, there are *two* peaks in the amplitude of nanowall's oscillations that occur at 0.7 THz (low-frequency peak) and at 3.2 THz (high-frequency peak). Existence of these peaks suggests that the nanowalls exhibit a resonance dynamics and must have a mass associated with them.

We develop a general theory of nanowall dynamics. Since a nanowall behaves as an elastic object, we use the mathematical model of a damped harmonic oscillator to postulate the nanowall's response function $\alpha(t) = \gamma e^{-\frac{t}{\tau}} \cos(\omega_0 t + \psi)$, where γ and ψ are parameters to be determined later, τ is relaxation time, ω_0 is the intrinsic, or characteristic, frequency of

the nanowall. The response function describes the response of the domain wall to a delta-function excitation and incorporates two mechanisms: exponential relaxation and elastic vibrations near the equilibrium position. The exponential relaxation occurs if the dipoles near the domain walls can be considered as rigid and flip under the application of an electric field with the probability proportional to $1-e^{-t/\tau}$. Elastic vibrations of the domain wall may occur if the dipoles near the domain boundary behave as elastically bound charges that may exchange their positions during elastic vibrations. Convolution of the response function with "step-down" electric field gives a decay function which describes how a displaced nanowall attains equilibrium position after the external field is suddenly removed. For our $\alpha(t)$ the decay function is $\Delta X(t) \sim e^{-\frac{t}{\tau}} \cos(\omega_0 t)$. While the response function contains complete information about the dynamics of the domain wall, it cannot be directly obtained from the domains dynamics under an *ac* electric field. We will, therefore, use a complex response function $\eta(w) = \int_0^\infty \alpha(t) e^{i\omega t} dt$ that describes the nanowall's response to an *ac* electric field E: $\Delta X = \eta(w)E$. Following the standard integration technique [22] we obtain

$$\eta(w) = \frac{1}{2}\Delta\eta \left(\frac{1 - i\omega_0\tau}{1 - i(\omega_0 + \omega)\tau} + \frac{1 + i\omega_0\tau}{1 + i(\omega_0 - \omega)\tau} \right) \tag{1}$$

where $\Delta\eta = \gamma\tau\cos\psi$ and $\omega_0\tau = -\tan\psi$. Fitting our numerical data from Fig.2 using the analytical function of Eq.(1) will reveal if a nanowall indeed moves as an elastic object, in which case the fitting parameters ω_0, τ, $\Delta\eta$ will determine the nanowall's response function $\alpha(t)$.

A sum of two analytical functions $\eta_1(w) + \eta_2(w)$ is used to simultaneously fit low- and high-frequency processes (indexes 1 and 2, respectively) associated with the two peaks in $X(\omega)$. For the thinnest film we obtained $\nu_{0,1} = \omega_{0,1}/2\pi = 0.95$ THz, $\nu_{0,2} = 3.00$ THz, $\tau_1 = 0.29$ ps, $\tau_2 = 0.36$ ps, $\Delta\eta_1|E| = 0.5$ nm, $\Delta\eta_2|E| = 0.05$ nm [28]. The ratios $\nu_{0,i}/\tau_i$ indicate that low- (high-) frequency process behaves as a damped (underdamped) harmonic oscillator.

Figs.3(a)-(c) give the characteristic parameters $\omega_{0,i}$, τ_i, $\Delta\eta_i$ for all other films. We first focus on the high-frequency process (shown with diamonds). The characteristic frequency of this process increases with the film's thickness and stabilizes around 4.7 THz. This coincides with the frequency of A_1 mode [23] and suggests that the high-frequency process is associated with the soft mode dynamics, or the dynamics of individual dipoles. This dynamics is intrinsic to the material and independent of domains. In additional calculations we indeed

find that the characteristic frequencies of the dipoles in the films are very close to $w_{0,2}$. This confirms that the high-frequency process is associated with the intrinsic dipoles' dynamics in the soft mode, which couples to the electric field to produce large resonance vibrations. The dipole's vibrations near the nanowalls facilitate the dipoles' flip and, therefore, contribute to the domain wall dynamics. Overall, high-frequency process contributes about 10% to the nanowall's dynamics.

We next focus on the low-frequency process (shown with squares in Figs.3(a)-(c)). The intrinsic frequency $\omega_{0,1}$ of such process decreases rapidly with the film's thickness and vanishes at the critical thickness of 7.4 nm. By substituting $\omega_0 = 0$ in Eq.(1) we obtain the complex response function for thicker films $\eta(w) = \frac{\Delta\eta}{1-i\omega\tau}$ which describes Debye relaxation. Debye relaxation is usually found in materials with order-disorder dynamics. In other words, a film undergoes an exotic size-driven transition from resonance to relaxational dynamics at a critical thickness of 7.4 nm. Moreover, the transition is gradual as evident from a comparison of normalized decay functions plotted for films of different thicknesses (Fig.3(d)). The dynamics embodied in these plots is striking: a displaced nanowall in a thin film will make a few oscillations before returning to its equilibrium position, while a nanowall in a thicker film will relax exponentially to its equilibrium position.

To identify the driving force for such an unusual transition we calculate the mass of a nanowall. It was proposed [24] that the effective mass of a domain wall can be estimated from the kinetic energy of ions in those dipoles that flip as the wall propagates. Using similar arguments we derived a formula for a nanowall's mass per unit area a^2: $M_{NW} = m(< q_z > /Z^*a)^2$, where m and Z^* are the ionic mass and charge of a dipole, and a is the lattice constant. This formula suggests that the nanowall's mass is not constant but follows the size dependence of $< q_z >$ (see Fig.1(b)). Therefore, at nanoscale the domain wall mass becomes a size and/or shape property rather than just a material property. As the thickness of the film increases, the mass of the nanowall increases as well (Fig.3(e)). In the elastic regime the characteristic frequency of a nanowall is inversely proportional to the nanowall's mass, which explains the decrease in $w_{0,1}$ that occurs for thinner films (Fig.3(b)). For films thicker than 7.4 nm, the nanowall becomes too heavy thereby causing the film to transition into relaxational dynamics.

To confirm whether the type of the oscillatory dynamics is determined by the nanowall's mass, we conduct additional calculations on a 13 nm film ($M_{NW} = 2.2 \cdot 10^{-9}$ kg/m^2). Our

aim is to convert the dynamics of this film from relaxation to resonance by reducing M_{NW} in two different ways: (a) decreasing the ionic masses in the local dipole to yield $M_{NW} = 1.3 \cdot 10^{-9}$ kg/m^2; (b) reducing $< q_z >$ to yield $M_{NW} = 0.8 \cdot 10^{-9}$ kg/m^2 [29]. In both cases the film was indeed converted into resonance dynamics as evident from the decay functions plotted in Fig.3(f). We therefore conclude that the nanowall's dynamics is controlled by the nanowall's mass, which in turn depends on the nanodomain size [30].

Fig.3(a) shows that in the relaxation regime τ_1 increases linearly with the film thickness which suggests that the dispersion frequency (which is inversely proportional to the relaxation time) should decrease as the film thickness increases. Extrapolation of our data to millimeter thicknesses [31] yields dispersion frequencies in the GHz range, which is in good agreement with some experimental and theoretical findings [25].

We next discuss how domain propagation occurs at nanoscale. For many decades it was believed that in bulk domains propagate through nucleation and growth of a triangular nucleus. Recently however a model of a small square nucleus was proposed [14]. In utrathin films the domain propagation is not described by any of these models but rather has its own unique pattern. We found that the nanowall propagates inhomogeneously with polarization reversal originating at the surface of the film and then advancing into its interior. This can be traced to a depolarizing field which rotates the surface dipoles in-plane to annihilate the open flux (see the domain closure pattern in Fig.1(a),(c),(d)). As a result the surface dipoles have the smallest out-of-plane component and, therefore, are easiest to flip.

We repeated all simulations in the presence of dynamical deformations that compress/stretch the films periodically along the out-of-plane direction. Such deformations may be caused by the vibrations of the substrate, laser pulses or dynamical change of stresses. The deformation is modeled as a periodic variation of the out-of-plane lattice constant $c(t) = c_{eq} + \Delta c \sin(\omega_c t + \chi)$, where c_{eq} and Δc are the equilibrium lattice constant and the amplitude of the deviation from c_{eq}, ω_c is the frequency of the periodic load, and χ is a phase-shift with respect to electric field. For all the films we observe a sharp peak in the displacement $X(\omega)$ at $\omega = 0.5\omega_c$ (see Fig.4), which can be explained as follows. In the absence of any electric field the out-of-plane dipole component $|q_z|$ is maximized when c is at maximum, or $\omega_c t + \chi = \frac{\pi}{2} + 2\pi n$ (piezoelectric coupling). On the other hand, under an *ac* electric field, but in the absence of dynamical load, $|q_z| \sim |\sin(\omega t)|$ and is maximized at $\omega t = \frac{\pi}{2} + \pi m$. Both maximums occur at the same time if $\omega = 0.5\omega_c$ and will cause

resonance vibrations. Such dynamical coupling can find useful applications in ultrasensitive nanomechanical sensors.

In summary, we have studied the intrinsic nanodynamics of ferroelectric ultrathin films with nanodomains. Our first-principles-based insight revealed that such nanodynamics is qualitatively different from the dynamics at larger scale and exhibit numerous exotic phenomena. Surprisingly, some of them, such as dynamical coupling, may even be used in future superior nanodevices.

Acknowledgments: The present work is supported by the U.S. Department of Energy, Office of Basic Energy Sciences, Division of Materials Sciences and Engineering under award DE-SC0005245 (computational studies) and by USF under Grant No. R070699 (some theoretical developments). The use of services provided by Research Computing, USF is greatly acknowledged.

---

* Electronic address: iponomar@usf.edu

[1] J. Junquera and P. Ghosez, Nature (London) **422**, 506 (2003).

[2] D. Fong et al., Science **304**, 1650 (2004).

[3] I. Naumov, L. Bellaiche, and H. Fu, Nature (London) **432**, 737 (2004).

[4] I. Ponomareva and L. Bellaiche, Phys. Rev. B **74**, 064102 (2006).

[5] J. F. Scott and C. A. P. de Araujo, Science **246**, 1400 (1989).

[6] J. F. Scott, J. Phys.: Condens. Matter **18**, R361 (2006).

[7] J. Scott, Science **315**, 954 (2007).

[8] M. Dawber, K. M. Rabe, and J. F. Scott, Rev. Mod. Phys. **77**, 1083 (2005).

[9] I. Kornev, H. Fu, and L. Bellaiche, Phys. Rev. Lett. **93**, 196104 (2004).

[10] S. Lisenkov, I. Ponomareva, and L. Bellaiche, Phys. Rev. B **79**, 024101 (2009).

[11] B.-K. Lai, I. Ponomareva, I. Kornev, L. Bellaiche, and G. Salamo, Appl. Phys. Lett. **91**, 152909 (2007).

[12] B.-K. Lai, I. Ponomareva, I. Naumov, I. Kornev, H. Fu, L. Bellaiche, and G. Salamo, Phys. Rev. Lett. **96**, 137602 (2006).

[13] W. J. Merz, Phys. Rev. **95**, 690 (1954).

[14] Y.-H. Shin, I. Grinberg, I.-W. Chen, and A. M. Rappe, Nature **449**, 881 (2007).

[15] K. Uchino, Ferroelectric devices (Marcel Dekker, Inc., New York-Basel, 2000).

[16] L. Bellaiche, A. Garcia, and D. Vanderbilt, Phys. Rev. Lett. **84**, 5427 (2000).

[17] L. Bellaiche, A. Garcia, and D. Vanderbilt, Ferroelectrics **266**, 41 (2002).

[18] I. Ponomareva, I. I. Naumov, I. Kornev, H. Fu, and L. Bellaiche, Phys. Rev. B **72**, 140102 (2005).

[19] I. Ponomareva and L. Bellaiche, Phys. Rev. Lett. **101**, 197602 (2008).

[20] D. Rapaport, The Art of Molecular Dynamics Simulation (Cambridge University Press, 2001).

[21] I. Ponomareva, L. Bellaiche, T. Ostapchuk, J. Hlinka, and J. Petzelt, Phys. Rev. B **77**, 012102 (2008).

[22] H. Fröhlich, Theory of dielectrics: Dielectric constant and dielectric loss (Oxford at the Clarendon press, 1963).

[23] V. Sivasubramaniany, V. Murthyy, B. Viswanathanz, and M. Sieskindx, J. Phys.: Condens. Matter **8**, 2447 (1996).

[24] C. Kittel, Phys. Rev. **83**, 458 (1951).

[25] J. C. Burfoot, Ferroelectrics: an introduction to the physical principles (London, Princeton, N.J., Van Nostrand, 1967).

[26] Note that the oxygen octahedra degrees of freedom are not included in the present simulations. Since they do not directly couple with an electric field we do not expect them to play an important role in the nanowalls dynamics under an applied electric field.

[27] The amplitude of the electric fields depends on the film thickness and was chosen to satisfy two conditions: 1) avoid saturation - the point at which all the dipoles in a domain flip; 2) provide the same sweeping ratio V_{sweep}/V_{equil} for nanodomains belonging to different films. Here V_{sweep} and V_{equil} are the volume swept out by the oscillating nanowall and the volume of the nanodomain at equilibrium, respectively. Technically, the simulated fields were in the range of 150-1000 MV/m.

[28] Note that the fitting quality suggests that the low- and high-frequency processes are likely coupled.

[29] This was achieved by applying compressive strain along the film's out-of-plane direction.

[30] In the presence of defects we expect our qualitative conclusions to hold at least in the pinning-depinning and flow regions.

[31] Note, that all the reported features of the dynamics are intrinsic to nanoscale and extrapolation to other scales is speculative.

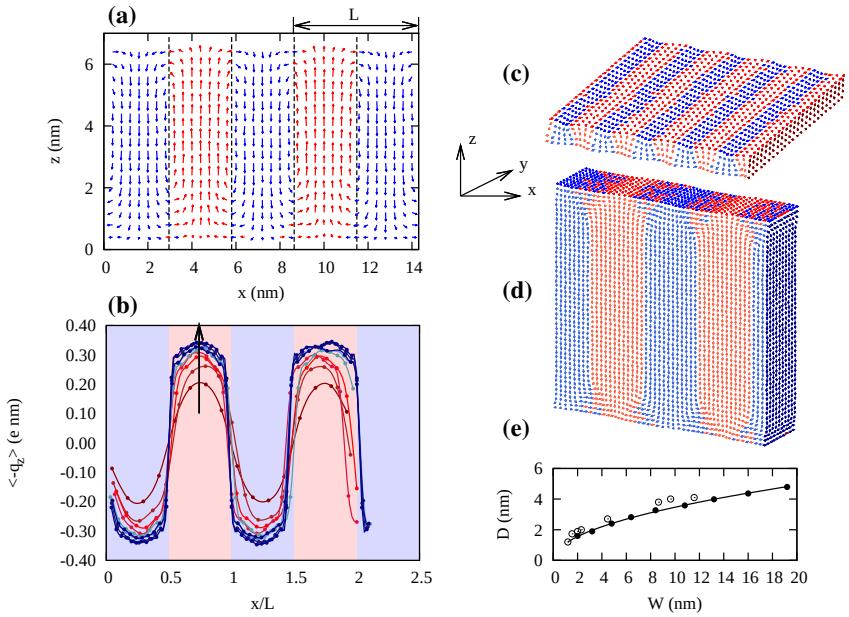

FIG. 1: (color online). Domains morphology. (a) Two-dimensional dipole pattern in a cross-section of 6.4 nm thick film. Dashed lines indicate the nanowalls. (b) Dipole moment profiles $< q_z(x/L) >$ for films with thicknesses 2, 3.2, 4.8, 6.4, 8.4, 10.8, 13.2, 16.0 and 19.2 nm. The average is taken over the dipoles having the same y- and z-coordinate. The arrow indicates the direction of the film thickness increase. (c) and (d) Three-dimensional slices of dipole patterns in 2 and 19.2 nm thick films, respectively. (e) The dependence of the domain width $D = L/2$ on the film thickness W. Solid circles represent our computational data, while empty circles represent experimental data for F_α phase from Ref.[2]. The line gives the square root fit for the computational data.

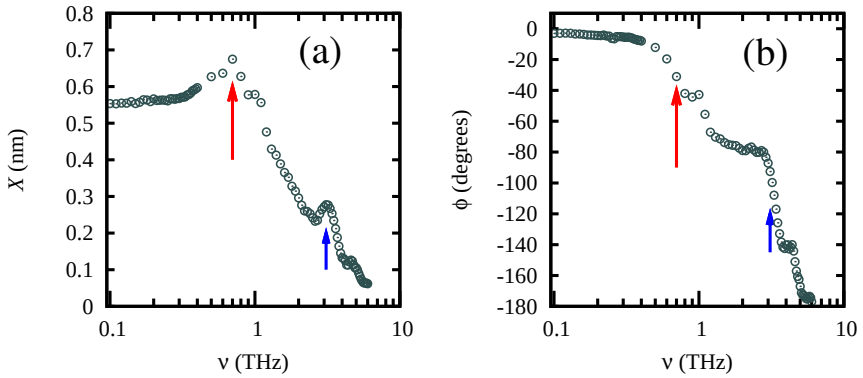

FIG. 2: (color online). Frequency dependent response of a nanowall to the electric field in a 0.2 nm thick film. The arrows indicate positions of the peaks.

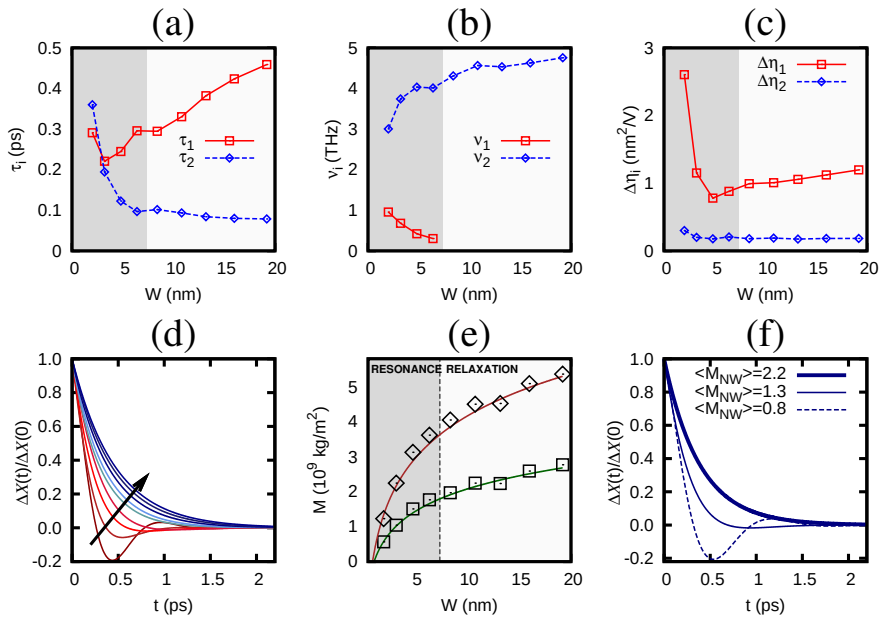

FIG. 3: (color online). Characteristic parameters of the nanowalls' dynamics. Relaxation times τ_i, intrinsic frequencies $\omega_{0,i}$ and response strengths $\Delta\eta_i$ are plotted as functions of film thickness in panels (a), (b) and (c), respectively. (d) Normalized decay functions for films. The arrow indicates the direction of the film thickness increase. (e) Nanowall mass as a function of the film thickness. Diamonds represent the masses calculated using the average dipole moments in the whole nanodomain, while squares represent the masses calculated using the average dipole moments near the nanowall. The later one is used for further analysis. (f) Decay functions for 13.2 nm thick film as obtained from calculations where the nanowall's mass is varied. The nanowalls masses are given in units of 10^9 kg/m^2.

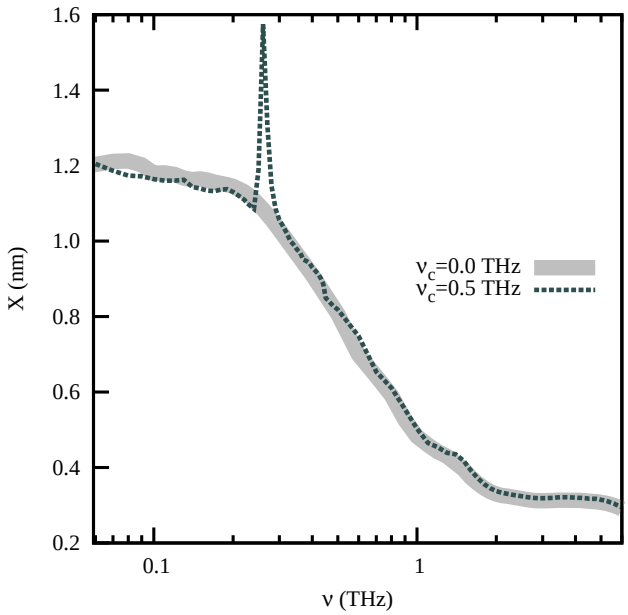

FIG. 4: (color online). The nanowall's displacement in 13.2 nm thick film as a function of the frequency of an *ac* electric field in the presence (dashed line) and absence (thick solid line) of dynamical vibrations.